Experimental Evaluation of 5G Modulation Schemes in Quasi-Static Scenarios

Tomás Domínguez-Bolaño, José Rodríguez-Piñeiro, José A. García-Naya, and Luis Castedo
University of A Coruña, A Coruña, Spain
{tomas.bolano, j.rpineiro, jagarcia, luis}@udc.es

***Abstract*—Orthogonal Frequency-Division Multiplexing (OFDM) is a widely used modulation scheme in wireless communications due to its robustness against channel multi-path. Unfortunately, the time-domain rectangular-shape of the OFDM-modulated symbols yields an infinitely long frequency response, thus producing co-channel interference. More recently, Filter Bank Multicarrier (FBMC) modulation schemes have been proposed as an alternative to OFDM due to its better spectral efficiency and more degrees of freedom to define well localized prototype filters.**

In this paper, the performance of two common prototype filters for an FBMC scheme, known also as Staggered Multitone (SMT), is analyzed analytically and by means of computer simulations considering standardized channel models. The results are also compared to OFDM. Finally it is experimentally evaluated through over-the-air transmissions in different environments using a custom-developed testbed. Simulation results, in terms of the Bit Error Ratio (BER) with respect to the average transmit power divided by the noise variance, show a similar performance for OFDM and FBMC. This is mainly because the considered channel models are quasi-static and we have considered an isolated point-to-point link, thus not including potential advantages of FBMC schemes, which can be exploited without additional performance losses with respect to OFDM.

I. Introduction

Orthogonal Frequency-Division Multiplexing (OFDM) is currently one of the most used Multi Carrier Modulation (MCM) schemes for wireless communications. This is due to its several advantages, among which some of the most remarkable are its robustness against multi-path propagation (frequency-selective channels), and that it can be implemented very efficiently using an Inverse Fast Fourier Transform (IFFT) block at the transmitter, a Fast Fourier Transform (FFT) block at the receiver, and a single tap per subcarrier Zero-Forcing (ZF) equalizer. However, the robustness against multi-path channels is achieved by inserting a Cyclic Prefix (CP) to each OFDM symbol, which reduces the spectral efficiency, and the time-domain rectangular-shape of the symbols lead to an infinitely long frequency response.

Over the last few years, schemes based on Filter Bank Multicarrier (FBMC) using Offset Quadrature Amplitude Modulation (OQAM) have received some attention as a promising alternative to OFDM [1]. In OQAM a time-offset of half the Quadrature Amplitude Modulation (QAM) symbol duration is introduced between the real and the imaginary parts. These systems are known as FBMC/OQAM or OFDM/OQAM [2]. The more concise name Staggered Multitone (SMT) has also been suggested recently [1].

Compared to OFDM, SMT systems do not use a CP, so they may provide a higher useful bit rate. The considered prototype filter can be adapted to the time and frequency dispersion characteristics of the given channel, thus these systems can offer a more localized frequency response, yielding a better performance in some situations (e.g. doubly dispersive channels). Finally, SMT systems can be also implemented efficiently using an IFFT block at the transmitter and a FFT block at the receiver [3].

However, channel estimation in SMT is more difficult than in OFDM. In OFDM scattered pilots are commonly inserted among the data symbols and, since the OFDM symbols are orthogonal, the pilot symbols can be recovered ideally without interference and the channel can be estimated easily. In SMT, the real and imaginary parts of the QAM symbols are separated and transmitted as a pair of Pulse Amplitude Modulation (PAM) symbols, but unlike OFDM, the orthogonality only holds for the real part [4]. The symbols recovered at the receiver are complex-valued and the imaginary part is due to the channel effect plus interferences from the surrounding symbols. Hence the channel cannot be estimated directly even in the case of an ideal channel. To overcome this problem, several channel estimation methods have been proposed in the literature. In [4], one symbol adjacent to each pilot is employed to cancel the imaginary interference. This adjacent symbol was named later in [5] as Auxiliary Pilot (AP). More recently [6], a more complex method named Coded Auxiliary Pilot (CAP) was proposed. This method is based on the same idea of canceling the interference, but in this case a linear coding is applied to the data symbols surrounding the pilot. As shown in [6], the AP takes up a significant amount of power overhead to cancel the interference, which can be reduced significantly by applying the proposed CAP method.

Several comparisons between the performance of OFDM and FBMC are available in the literature [7]–[10]. However, to the best knowledge of the authors, most of them are solely based on analytic and/or simulation-based results. The main contribution of this paper is the experimental evaluation (by means of over-the-air transmissions) of two of the proposed prototype filters for SMT systems, namely the one defined by the PHYDYAS project [11] and the so-called Hermite pulse [12]. Performance will be evaluated over quasi-static scenarios in terms of Bit Error Ratio (BER) against the transmit power. The performance of OFDM will also be included for comparison purposes. Simulation results based on channel models standardized by the 3rd Generation Partnership Project (3GPP) are also included.

II. SMT Signal Model

In this section we describe the signal model used in our simulations and experimental evaluations. We consider a SMT scheme using N subcarriers and transmitting P time-domain symbols per subcarrier. We denote $\mathcal{A}$ as the set of subcarriers utilized by the system, with values between 0 and $N-1$.

The discrete-time baseband SMT modulated signal is

$$s[k]=\sum_{p=0}^{P-1}\sum_{l\in\mathcal{A}}a_{l,p}g\left[k-p\frac{N}{2}\right]\exp\left(j\phi_{l,p}\right)\exp\left(jl\frac{2\pi}{N}k\right),$$

where $g[k]$ is the discrete-time prototype filter used, $a_{l,p}$ is the transmitted PAM symbol for time p and subcarrier l, and $\phi_{l,p}=\frac{\pi}{2}\left(l+p\right)$.

The signal $s[k]$ is sent by the transmitter, passes through a physical channel and is affected by Additive White Gaussian Noise (AWGN) resulting in the received signal $r[k]$, which is modeled as

$$r[k]=\sum_{\tau}h[k,\tau]*s[k-\tau]+w[k],$$

where $h[k,\tau]$ is the discrete-time channel impulse response, $w[k]$ is the uncorrelated complex-valued AWGN with variance σ_w^2, and $*$ denotes the convolution operation.

For each subcarrier m at the receiver, $r[k]$ is first down-converted multiplying by $\exp\left(-jm\frac{2\pi}{N}k\right)$ and filtered by the matched filter $\hat{g}[k]$ to obtain the signal

$$y_m[k]=r[k]\exp\left(-jm\frac{2\pi}{N}k\right)*\hat{g}[k].$$

Finally, the symbols $a_{l,p}$ are recovered as

$$\hat{a}_{l,p}=\Re\left\{\exp\left(-j\phi_{l,p}\right)y_l\left[p\frac{N}{2}\right]\right\}.$$

For our evaluations, we consider $g[k]$ as the prototype filters defined by the PHYDYAS project [11] and the so-called Hermite pulse [12]. For these filters the receiver matched filter will be the same as the transmitter filter, i.e., $\hat{g}[k]=g[k]$, since they are symmetric in the time domain.

III. Evaluation Setup

We use the evaluation setup shown in Fig. 1. Two main branches can be distinguished, labeled as "measurements branch" and "simulations branch". On the one hand, the "measurements branch" implies using the GTEC Testbed (see Section III-C) to measure through an actual wireless channel. On the other hand, the "simulations branch" only includes a channel model, with the purpose of performing evaluations by simulations.

A. Signal Generation and Signal Processing

In this section, the high-level software part of the setup used for the evaluations is introduced, namely the blocks labeled "signal generation" and "signal processing".

At the transmitter side, SMT-modulated signals are generated using a custom-developed SMT signal generator. As mentioned earlier, the PHYDYAS project pulse [11] and the Hermite pulse [12] were implemented. It is worth noting that the latter is specially suited for multicarrier transmissions over doubly dispersive channels since it minimizes both the Inter-Carrier Interference (ICI) and the Inter-Symbol Interference (ISI) by means of a good localization in time and frequency [12]. Our signal generator also supports OFDM signals (which correspond to the use of a rectangular filter in the time domain). At the receiver side, a custom-developed SMT receiver is used. Such a receiver includes:

- **Basic channel estimation**: the channel response is estimated by means of a grid of pilots. For SMT signals, the receiver has to deal with the interference caused by the lack of orthogonality of the received signal, since only orthogonality in the real part is ensured [1]. Several methods that minimize the effect of the interference based on the so-called auxiliary pilot schemes were implemented [4]–[6]. For the results shown in this paper, the so-called CAP method [6] (using 8 symbols around each pilot) was considered.
- **Basic channel interpolation**: two-dimensional (time and frequency) interpolation techniques are used. More specifically, an interpolator based on the use of cubic splines is used.
- **Basic channel equalization**: a basic ZF equalizer was implemented.

Time and frequency synchronization algorithms are also implemented. However, in order to avoid distorting the results shown in this paper, perfect time and frequency synchronization was considered for the simulations.

B. Channel Model

Channel models were used to perform the evaluations based on simulations. We select noise variance values that lead to the desired P_T/σ_w^2 values, where P_T and σ_w^2 denote the transmitted power and the noise variance, respectively. The following channel models are considered: the Typical Urban channel model (TUx) for deployment evaluation specified by the 3GPP [13]; Indoor Office B (IBx) and Outdoor-to-Indoor and Pedestrian A (PAx), both from the ITU Radiocommunication Sector (ITU-R) third generation (3G) channel models [14]. The Doppler spread parameter of the channel models was set according to the carrier frequency as well as the desired speed. We consider static scenarios (0 km/h) as well as pedestrian mobility (3 km/h). While the TUx models situations in which the receiver is in a urban area, the IBx is more suitable for indoor transmissions. Finally, the PAx considers an outdoor-to-indoor scenario. These scenarios are the most typical ones for a pedestrian user.

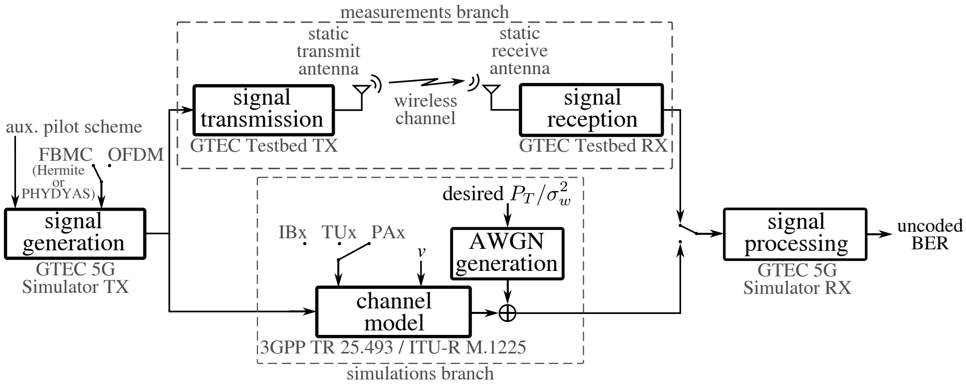

Fig. 1. Block diagram of the setup used for the evaluations. Notice that analytic performance results are also obtained considering AWGN and Rayleigh channel.

C. Testbed Description

The experimental evaluations described in this work are carried out with the testbed developed at our research group and used in previous works [15], [16]. More specifically, we employ two nodes: a transmit-only node and a receive-only node. Each node consists of a USRP B210 board [17] built from the AD9361 chip [18] by Analog Devices, which supports a continuous frequency coverage from 70 MHz to 6 GHz; full-duplex Multiple-Input, Multiple-Output (MIMO) operation with up to two antennas, and a maximum bandwidth of 56 MHz; USB 3.0 connectivity; on-chip 12 bit Analog-to-Digital Converters (ADCs) and Digital-to-Analog Converters (DACs) up to 61.44 Msample/s; and configurable transmit and receive gain values. For each node, its corresponding USRP board is connected to a laptop equipped with two solid-state drives: one containing a GNU/Linux operating system and the custom-developed measurement software, whereas the other is dedicated to storing the transmit/acquired signals.

The differences between the transmitter and the receiver nodes are, on the one hand, the two Mini-Circuits TVA-11-422 high-power amplifiers [19] and the two Ubiquity AM-2G15-120 cross polarized antennas [20] employed at the transmitter side. On the other hand, ultra-wideband and omnidirectional Taoglas GA.110.101111 antennas [21], with about 3 dBi gain, are employed at the receiver (they can also be used at the transmitter side).

With respect to the measurement software, we use a custom-developed multi-threaded software implemented in C++ with Boost [22] and based on the Ettus USRP Hardware Driver (UHD) [23]. At the transmitter side, the samples are first pre-processed and saved into a dedicated solid-state drive. Next, such samples are transmitted over the air in a cyclic fashion using a single antenna at a time from the set of four available. Switching the transmit antenna allows for obtaining different channel realizations from distinct spatial positions and polarizations. At the receiver, the samples coming out of the two antennas of the USRP are read from the USB and stored first in memory, and eventually recorded in a solid state drive. Other important logging information is also stored. Notice that the receiver node acquires signals simultaneously from two different antennas although a Single-Input Single-Output (SISO) system is being assessed.

D. Scenario of the Measurements

In this work we restrict the experimental evaluation to quasi-static scenarios. More specifically, we consider the following scenarios:

- A medium-size office represented by the laboratory of our research group at the University of A Coruña. The laboratory is located in the second floor of a building with coordinates $43°19'59.3''$ N, $8°24'33.2''$ W and it occupies an area of $82\,\mathrm{m}^2$.
- A small office with approximately $19\,\mathrm{m}^2$, represented by a room in the third floor of the aforementioned building, located above the laboratory.
- Corridors. Large buildings usually have corridors, which exhibit specific propagation conditions for wireless signals. Therefore, we also consider corridors as typical indoor scenarios.
- An outdoor-to-indoor scenario obtained by placing the transmitter outside the building while the receiver stays inside the laboratory.

In case of small and medium-size offices, both line-of-sight and non-line-of-sight links are considered. Additionally, measurements are carried out with both transmitter and receiver in static conditions, and also with the receiver moving at approximately 3 km/h.

More details, including pictures, of the measurement scenarios will be included in the final version of the manuscript.

IV. Evaluation Procedure

A. Ensuring a Fair Comparison

In order to fairly compare the results for the different considered modulations (OFDM and SMT with Hermite and PHYDYAS pulses), the following aspects were also considered:

- The number of data subcarriers, as well as the subcarrier spacing, are the same in all cases. More specifically, 600 subcarriers are used, while the subcarrier spacing was set to 15 kHz (for the OFDM case, 600 subcarriers are used for a 1024-point FFT). These parameters correspond to the typical configuration for the 10 MHz downlink Long Term Evolution (LTE) profile.

- The pilot density considered for channel estimation is equivalent in all cases. Note that in the case of SMT some additional symbols, namely the APs, are required to minimize the interference caused by the lack of orthogonality of the received pilots [1]. More specifically, a rectangular grid of pilots was used. Such pilot spacing in the time-frequency grid is of 8 subcarriers in the frequency dimension and of 10 symbols in the time dimension for SMT signals (5 symbols in the case of OFDM given that consecutive symbols do not overlap).
- The same algorithms for channel estimation, interpolation and equalization are considered for each of the modulations (see Section III-A).
- A 2-PAM constellation is used for the SMT transmissions, while 4-QAM is considered for OFDM, since the symbols are complex-valued in the latter case.
- Approximately the same number of user data bits is considered per transmission. Taking into account that real-valued symbols are used in SMT, whereas complex-valued ones are used for OFDM, more time-positions in the time-frequency grid are required for SMT signals with respect to OFDM for the same number of transmitted bits. However, provided that consecutive SMT symbols partially overlap in the time domain (because a SMT scheme is considered), this does not mean that in order to transmit the same amount of data bits we need twice the time-positions for SMT with respect to OFDM. With model the considered, the user bit rate is approximately equivalent for both OFDM and SMT, with slight differences caused by the length of the OFDM cyclic prefix and the time dispersion of the prototype filters in SMT.
- The signals are scaled to ensure that the transmitted energy per bit is equivalent for both OFDM and SMT.

We consider the uncoded BER (i.e., the BER after the symbol hard-decision) as the figure of merit for the results evaluation, since it is one of the most used performance metrics in wireless communications.

Finally, Table I details the most relevant parameters considered.

B. Measurement Procedure

Taking advantage of the antenna switching capabilities exhibited by the USRP B210 board and that a SISO system is being considered, eight different channel realizations can be measured without moving the transmit nor the receive node. More channel realizations can be easily obtained by moving the transmitter and the receiver in a small area (typically of $3\,\lambda \times 3\,\lambda$ [24], where λ is the wavelength).

In order to ensure a fair comparison, all waveforms under test are transmitted sequentially under the same conditions (notice that we are assuming quasi-static wireless channels).

More details about the exact procedure and involved configuration parameters will be provided in the final version of the manuscript.

TABLE I
MAIN PARAMETERS USED IN THE EXPERIMENTS.

parameter	**value**
Sampling frequency, F_s	15.36 MHz
FFT size	1024
Number of used subcarriers	600 (excluding DC)
CP length (OFDM)	72 samples
Constellations	2-PAM (SMT) 4-QAM (OFDM)
Pilot spacing	8 subcarriers (frequency dimension) 10 symbols (time dimension, SMT) 5 symbols (time dimension, OFDM)
AP scheme	CAP (8 surrounding symbols)
Pulse overlapping	3 symbols (Hermite) 4 symbols (PHYDYAS)
Velocities, v	0, 3 km/h
Carrier frequency, f_c	2.5 GHz
P_T/σ_w^2	from 0 to 30 dB

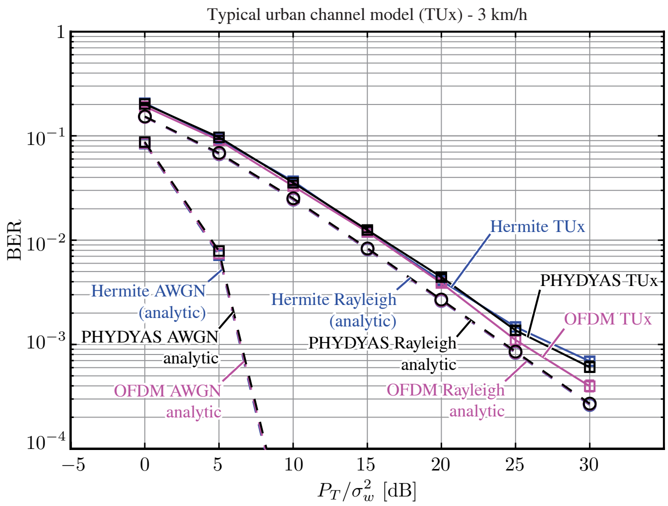

Fig. 2. BER versus P_T/σ_w^2 for the TUx channel model. Pedestrian mobility (3 km/h) is considered.

V. SIMULATION RESULTS

All the results included in this section are expressed in terms of BER with respect to the P_T/σ_w^2, where P_T is the average transmit power, and σ_w^2 is the noise variance. With the objective of gauging the accuracy of the results, 95 % confidence intervals are also included.

- Fig. 2 shows the BER versus P_T/σ_w^2 for the TUx channel model when Pedestrian mobility ($v = 3$ km/h) is considered. Additionally, the analytic curves for the three systems (i.e., OFDM and SMT with PHYDYAS and Hermite pulses) considering both AWGN and Rayleigh channel models. The curves corresponding to the analytic models (assuming perfect channel knowledge) show that the comparison is fair since they almost completely overlap. The BER exhibited by the rest of the curves is almost the same (less than 2 dB) for P_T/σ_w^2 values smaller

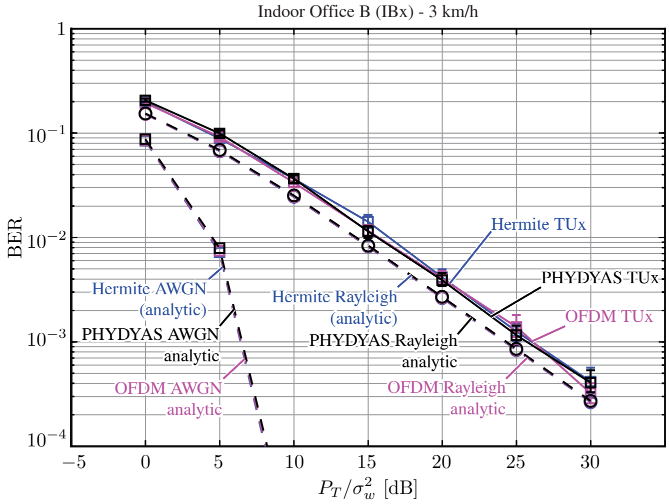

Fig. 3. BER versus P_T/σ_w^2 for the IBx channel model. Pedestrian mobility (3 km/h) is considered.

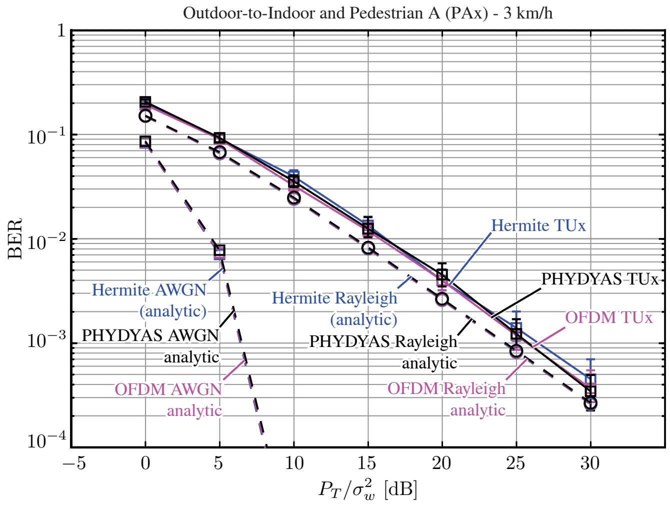

Fig. 4. BER versus P_T/σ_w^2 for the PAx channel model. Pedestrian mobility (3 km/h) is considered.

than 20 dB. For large P_T/σ_w^2 values ($P_T/\sigma_w^2 = 30$ dB), OFDM performs the best, followed by PHYDYAS, and finally Hermite. This is because the auxiliary pilots are designed for minimizing the interference when an ideal channel is considered. However, depending on the specific channel behavior, the interference caused by the pilot symbols at the receiver can be larger or smaller.

- Fig. 3 shows the same results as Fig. 2 but when the IBx channel model is considered. In this case all the schemes perform similarly because this channels can be equalized easier than those corresponding to the TUx model.
- Fig. 4 shows the same results as Figs. 2 and 3 but when the PAx channel model is considered. The comments for the case of Fig. 3 also apply here.

VI. Measurement Results

This section will be available in the final version of the manuscript.

VII. Conclusions

In this work we have compared the performance of two common prototype filters (the one defined by the PHYDYAS project, and the so-called Hermite pulse) for the widely proposed SMT scheme. The performance is expressed in terms of BER with respect to the P_T/σ_w^2, where P_T is the average transmit power and σ_w^2 is the noise variance at the receiver. In order to avoid impacting the results obtained by simulations, we considered perfect time and frequency synchronization between transmitter and receiver. A ZF channel equalizer was implemented at the receiver, and the TUx, IBx and PAx channel models were considered, assuming pedestrian mobility ($v = 3$ km/h). Additionally, analytic BER curves were also obtained for the AWGN and Rayleigh channel models with the purpose of ensuring a fair comparison among all the schemes.

The main conclusions derived from the simulation results are:

- A similar performance is obtained for the three schemes considered: OFDM, SMT with the PHYDYAS prototype filter, and SMT with the Hermite prototype filter.
- The spectral efficiency is very similar in all cases, which is confirmed by the analytic curves;
- The considered channel models are quasi-static and they are relatively easy to equalize. Hence, no significant difference between the performance of the distinct schemes can be appreciated in the simulation results. More specifically, the potential advantages of the Hermite prototype filter for doubly dispersive channels are not exploited in this case.
- The potential advantages of the FBMC schemes can be exploited, in quasi-static environments, without additional performance losses with respect to OFDM.

The conclusions related to the measurement results will be provided in the final version of the manuscript.

ACKNOWLEDGMENT

This work has been funded by Xunta de Galicia, MINECO of Spain, and FEDER funds of the EU under grants with numbers 2012/287, TEC2013-47141-C4-1-R, FPU12/04139, EST14/00355, BES-2014-069772.

REFERENCES

[1] B. Farhang-Boroujeny, "Ofdm versus filter bank multicarrier," *Signal Processing Magazine, IEEE*, vol. 28, no. 3, pp. 92–112, 2011.

[2] B. L. Floch, M. Alard, and C. Berrou, "Coded orthogonal frequency division multiplex [tv broadcasting]," *Proceedings of the IEEE*, vol. 83, no. 6, pp. 982–996, 1995.

[3] A. Sahin, I. Guvenc, and H. Arslan, "A survey on multicarrier communications: Prototype filters, lattice structures, and implementation aspects," *Communications Surveys & Tutorials, IEEE*, vol. 16, no. 3, pp. 1312–1338, 2012.

[4] J.-P. Javaudin, D. Lacroix, and A. Rouxel, "Pilot-aided channel estimation for ofdm/oqam," in *Vehicular Technology Conference, 2003. VTC 2003-Spring. The 57th IEEE Semiannual*, vol. 3. IEEE, 2003, pp. 1581–1585.

[5] T. H. Stitz, T. Ihalainen, A. Viholainen, and M. Renfors, "Pilot-based synchronization and equalization in filter bank multicarrier communications," *EURASIP Journal on Advances in Signal Processing*, vol. 2010, p. 9, 2010.

[6] W. Cui, D. Qu, T. Jiang, and B. Farhang-Boroujeny, "Coded auxiliary pilots for channel estimation in FBMC-OQAM systems," *IEEE Transactions on Vehicular Technology*, vol. PP, no. 99, pp. 1–1, 2015, doi:10.1109/TVT.2015.2448659.

[7] M. Fuhrwerk, J. Peissig, and M. Schellmann, "Performance comparison of CP-OFDM and OQAM-OFDM systems based on LTE parameters," in *IEEE 10th International Conference on Wireless and Mobile Computing, Networking and Communications (WiMob)*, Oct. 2014, pp. 604–610, doi:10.1109/WiMOB.2014.6962232.

[8] ——, "Channel adaptive pulse shaping for OQAM-OFDM systems," in *Proceedings of the 22nd European Signal Processing Conference (EUSIPCO)*. IEEE, 2014, pp. 181–185.

[9] M. Payaró, A. Pascual-Iserte, and M. Nájar, "Performance comparison between FBMC and OFDM in MIMO systems under channel uncertainty," in *European Wireless Conference (EW), 2010*. IEEE, 2010, pp. 1023–1030, doi:10.1109/EW.2010.5483521.

[10] I. Estella, A. Pascual-Iserte, and M. Payaró, "OFDM and FBMC performance comparison for multistream MIMO systems," in *Future Network and Mobile Summit, 2010*, Jun. 2010, pp. 1–8.

[11] M. Bellanger, D. Le Ruyet, D. Roviras, M. Terré, J. Nossek, L. Baltar, Q. Bai, D. Waldhauser, M. Renfors, T. Ihalainen *et al.*, "Fbmc physical layer: a primer," PHYDYAS FP7 Project Document, Tech. Rep., 2010.

[12] R. Haas and J.-C. Belfiore, "A time-frequency well-localized pulse for multiple carrier transmission," *Wireless Personal Communications*, vol. 5, no. 1, pp. 1–18, 1997.

[13] 3GPP, "3GPP TR 25.943: 3GPP;Technical specification group radio access network; Univerlsal Mobile Telecommunications System (UMTS); Deployment aspects," ETSI, Tech. Rep., December 2004.

[14] ITU-R, "Guidelines for evaluation of radio transmission technologies for IMT-2000. ITU-R Recommendation M.1225," 1997.

[15] J. Rodríguez-Piñeiro, P. Suárez-Casal, J. A. García-Naya, L. Castedo, C. Briso-Rodríguez, and J. I. Alonso-Montes, "Experimental validation of ICI-aware OFDM receivers under time-varying conditions," in *IEEE 8th Sensor Array and Multichannel Signal Processing Workshop (SAM 2014)*, A Coruña, Spain, June 2014.

[16] P. Suárez-Casal, J. Rodríguez-Piñeiro, J. A. García-Naya, and L. Castedo, "Experimental assessment of WiMAX transmissions under highly time-varying channels," in *he Eleventh International Symposium on Wireless Communication Systems (ISWCS)*, Barcelona, Spain, Aug. 2014.

[17] "Ettus USRP B210." [Online]. Available: https://www.ettus.com/product/details/UB210-KIT

[18] "Analog devices AD9361 RFIC." [Online]. Available: http://www.analog.com/en/rfif-components/rfif-transceivers/ad9361/products/product.html

[19] "Mini-circuits high-power amplifier TVA-11-422." [Online]. Available: http://www.minicircuits.com/pdfs/TVA-11-422.pdf

[20] "Ubiquity am-2g15-120 cross polarized antenna." [Online]. Available: http://dl.ubnt.com/datasheets/airmaxsector/airMAX_Sector_Antennas_DS.pdf

[21] "Taoglas m-2g15-120 ga.110.101111 omnidirectional antenna." [Online]. Available: http://taoglas.com/images/product_images/original_images/GA.110.101111.pdf

[22] "Boost C++ libraries." [Online]. Available: http://www.boost.org/

[23] "Ettus USRP hardware driver (UHD)." [Online]. Available: http://files.ettus.com/manual/page_uhd.html

[24] S. Caban, J. A. Garcia-Naya, and M. Rupp, "Measuring the physical layer performance of wireless communication systems: Part 33 in a series of tutorials on instrumentation and measurement," *IEEE Instrumentation and Measurement Magazine*, vol. 14, no. 5, pp. 8–17, Oct. 2011, doi:10.1109/MIM.2011.6041377.